Post-Print of an Accepted Manuscript on the Laboratory of Turbulent Flows Website

Complete citation:

Mohammadtabar, M., Sanders, R. S., & Ghaemi, S. (2020). Viscoelastic properties of flexible and rigid polymers for turbulent drag reduction. Journal of Non-Newtonian Fluid Mechanics, 283, 104347. doi: 10.1016/j.jnnfm.2020.104347

The final publication is available at https://doi.org/10.1016/j.jnnfm.2020.104347

Elsevier is the copyright holder; however, permission is granted to publicly share the preprint on any website or repository at any time.

The Accepted Manuscript begins on the next page.

Viscoelastic properties of flexible and rigid polymers for turbulent drag reduction

M. Mohammadtabar[1], R.S. Sanders[2], and S. Ghaemi[1,a)]

[1]*Department of Mechanical Engineering, University of Alberta, Edmonton, T6G 1H9, Canada*

[2]*Department of Chemical and Materials Engineering, University of Alberta, Edmonton, T6G 1H9, Canada*

The relation between the drag reduction (DR) performance of several water-soluble polymers and their viscoelastic properties was investigated. Polymers with a flexible molecular structure including three grades of polyacrylamides (PAM), and a polyethylene oxide (PEO) were investigated. Xanthan gum (XG) and carboxymethyl cellulose (CMC), each with a rigid molecular structure, were also considered. The rheology was characterized using steady shear-viscosity measurement, capillary break-up extensional rheometer (CaBER), and small-amplitude oscillatory shear measurement at the concentration of the drag-reduced solution. To isolate the effect of shear viscosity, the concentration of the polymers was adjusted to produce solutions with a similar shear viscosity at high shear rates. Using pressure drop measurements in a turbulent pipe flow, the DR of each polymer solution was determined. With identical high-shear-rate viscosities, the flexible PAM solutions resulted in an initial DR of 50-58%, while the initial DR of PEO was 44%, and the rigid polymers provided the least DR of 12%. The rigid polymers demonstrated negligible degradation of DR over a period of 2 hours. Of the flexible polymers, PAM showed moderate degradation, while the DR of PEO quickly diminished after 20 min. Drag reduction correlated with extensional viscosity and Weissenberg number obtained from CaBER. A strong correlation was not observed between DR and the viscoelastic moduli obtained from small-amplitude oscillatory shear. The large mechanical degradation of PEO was associated with a continuous extensional thickening, in which extensional viscosity increased with decreasing strain rate until the filament broke up.

[a] Author to whom correspondence should be addressed. Email: ghaemi@ualberta.ca

I. Introduction

Turbulent pipe flows play an important role in firefighting, irrigation, sewers, heating and cooling, and oil pipelines.[1] The higher drag of turbulent flows compared to laminar flow requires greater pumping power and results in a higher transportation cost. For this reason, reducing drag in turbulent pipe flows is of interest, and drag reduction (DR) methods using additives such as micro-bubbles, fibers, surfactants, and polymers have been investigated. Among these methods, the use of long-chain polymers has attracted more attention due to the small quantity of polymer required for DR. For example, Warholic et al.[2] observed 43% DR using 1.24 part per million (ppm) of a copolymer of polyacrylamide and sodium acrylic, while DR as large as 80% was obtained by Virk et al.[3] using 110 ppm of polyacrylamide.

The DR efficiency depends on several parameters, among others, such as concentration, molecular structure, chain flexibility, and molecular weight (MW) of the polymer, and solvent properties such as its temperature, pH, and salt content. There is a consensus in the literature regarding the effect of some of these parameters. It is known that DR increases monotonically with respect to polymer concentration up until an optimum concentration has been achieved. Above this concentration, DR decreases due to an increase in the solutions shear viscosity.[4,5] Virk[3] observed that polymers with a large molecular weight (i.e., longer chain) are often accompanied with large DR. The effect of temperature has been observed to depend on the structure of the polymer: when temperature was increased from 5 to 35ºC, Interthal et al.[6] observed that DR using polyethylene oxide (PEO) decreased from 70 to 50% while DR using polyacrylamide (PAM) did not change. Through extensive tests using a double-gap cylindrical geometry, Pereira et al.[7] observed that the variations of DR due to changes in concentration, molecular weight, and temperature for PAM and PEO are similar. The flexibility or rigidity of the polymer structure, also affects the DR. Examples of flexible polymers include PAM and PEO, while the typical rigid polymers used for DR include Xanthan gum (XG) and carboxymethyl cellulose (CMC). Pereira et al.[8] investigated the DR of dilute polymer solutions of PEO, PAM, and XG using the double-gap cylinder, and observed 21% and 19% DR using 25 ppm of flexible PEO and PAM polymers, while a smaller DR of 12% was achieved using XG at a similar concentration. The onset of DR and potentially the DR mechanism for flexible and rigid polymers are different. This has been shown by plotting the Fanning friction factor, f, in the Prandtl-von Kármán coordinate ($f^{-1/2}$ versus $Re \times f^{1/2}$).[9] For flexible polymers, the

data segments branch off the Prandtl-von Kármán line of the Newtonian turbulent flow (type A), while for the rigid polymers the segments come off the maximum DR asymptote (type B).[10, 11]

Two different mechanisms have been proposed to explain DR using polymers in turbulent flows. The first mechanism is based on larger viscous effects in a drag-reducing solution and the second mechanism is based on its elastic properties. Lumley[12] hypothesized that, due to the stretching of polymer molecules in a turbulent flow, the effective viscosity is large and damps the turbulence fluctuations.[1113] This hypothesis has been challenged since strain rate in a turbulent flow fluctuates, and therefore, the molecules can coil back when strain rate decreases.[14] De Gennes[15] proposed the second mechanism, in which DR is associated with the viscoelastic properties of the polymer solution. According to this theory, the partially stretched molecules absorb the turbulent kinetic energy in the near-wall region, and release it farther away from the wall where strain rate is small. This mechanism is hypothesized to terminate the turbulent energy cascade at a larger length-scale relative to the Kolmogorov scale of the Newtonian turbulent flow.[14] Therefore, in a drag-reducing solution, the smaller turbulence structures are believed to behave elastically; i.e. the small turbulence structures stretch and store the turbulent kinetic energy as an elastic energy.[14] However, these two DR mechanisms have been proposed for flexible polymers, and their applicability to rigid polymers with negligible chain flexibility is still an open question.[8] To evaluate this, the first step is to fully characterize the rheology of rigid and flexible polymer solutions in terms of effective viscosity and elasticity.

Many previous investigations have characterized polymer solutions using shear viscosity. This is perhaps due to the availability of equipment for measuring shear viscosity and the traditional characterization of non-Newtonian liquids using shear viscometers. However, shear viscosity appears to have little relevance to the two DR mechanisms proposed by Lumley[12] and Gennes[14]. A detailed review of the literature shows that there are only a few measurements in which viscoelastic properties have been characterized by small-amplitude oscillatory shear (SAOS) and filament-stretching rheometry. In addition, due to the lower measurement limit of the rheometers, these viscoelastic measurements were made at polymer concentrations at least an order of magnitude higher than that needed for maximum DR. Escudier et al.[16] observed that the DR of high concentration solutions of XG, CMC, and PAM (minimum of 2000 ppm) is proportional to their extensional viscosity at small shear rates (~10 1/s). This suggests a relationship between DR

and extensional viscosity; however, the polymer concentration was too large and the corresponding shear rate (i.e., ~10 1/s) is a few orders of magnitude smaller than the mean shear rate in a turbulent flow. These measurements were carried out using an opposed-nozzle rheometer which may not be accurate to obtain extensional visosity.[17] Japper-Jaafar et al.[10] used a capillary break-up extensional rheometer (CaBER) to characterize extensional viscosity by measuring the diameter of a thinning filament for non-ionic polysaccharide at concentrations of 1000 to 5000 ppm. From the filament diameter, they estimated the relaxation time (λ) and Trouton ratio (the ratio of extensional viscosity to shear viscosity). They observed a large Trouton ratio for all the polymer concentrations, which confirmed the dominance of non-Newtonian extensional behavior of the solutions. Pereira et al.[8] also used CaBER and observed a larger relaxation time for PEO than that of PAM at identical concentrations. They could not measure the relaxation time of XG since filament diameter did not follow the exponential decay proposed by Entov et al.[18]. Recently, Owolabi et al.[19] used CaBER for measurement of extensional viscosity in PAM solutions at low polymer concentrations (150-350 ppm), and investigated the variation of DR with Weissenberg number (*Wi*), defined as the product of λ and mean turbulent wall shear rate. They observed that DR rapidly increases with *Wi* and reaches an asymptote of about 64% when $Wi > 6$. A summary of the investigations reporting measurements of λ is presented in Table 1. The table shows that a limited number of extensional viscosity measurements have been reported, and that most of the measurements were made at concentrations higher than that needed for maximum drag reduction (MDR).

Oscillatory shear tests can measure the storage modulus (G') and the loss modulus (G'') to characterize the small-amplitude linear viscoelastic properties of a polymer solution. Nakken et al.[20] observed that G' and G'' moduli of a poly α-ofein polymer solution at 5000 ppm increased with increasing oscillation frequency from approximately 0.01 to 10 Hz. Pereira et al.[7] associated larger value of DR of PEO relative to PAM to a larger storage modulus (G') for oscillation frequency range of 0.01 to 10 Hz. However, to reduce measurement uncertainties, measurement of G' was conducted for a 10,000 ppm polymer solution while DR was measured at 2 to 50 ppm. Pereira et al.[8] also conducted oscillatory measurements for a wide range of concentrations that were higher than the concentration used for drag reduction measurement. For solutions with 10,000 ppm, they could carry out the oscillatory tests for a wide frequency range of 0.01 to 10 Hz. However, for solutions with a lower concentration of 1000 ppm, the oscillatory tests were limited to 0.08 to 0.8 Hz. Escudier et al.[21] used measurements of G' and G'' to identify the effect of solvent

and polymer preparation procedure on the rheology of the polymer solution. They measured the moduli for solutions with 4000 ppm of CMC and 2500 ppm of XG over frequency range of approximately 0.01 to 100 Hz. The oscillatory measurements of Japper-Jaafar et al.[10] for rigid polysaccharide solutions showed that G' is smaller than G'' when the polymer concentration is less than 2000 ppm (i.e., viscous dominated behavior), while G' is larger than G'' at higher concentrations (i.e., elastic dominated behavior). The observations were carried out at frequency range of 0.1 to 10 Hz. They also observed that the dependency of G' and G'' on frequency is smaller at higher concentrations. Wyatt et al.[22] showed that for a solution of XG at 60 ppm, the G' modulus, measured within 0.1 to 10 Hz, depends on the concentration of the master solution (varied from 500 to 10000 ppm). They observed that the greater the concentration of the master solution is, the larger are G' and DR. The change in DR was associated with the residual entanglements that are still sustained after diluting the concentrated master solution. A summary of the major investigations of oscillatory measurements, including solution concentration and the DR values are presented in Table 1. Except Wyatt et al.[22], all these investigations carried out SAOS measurements at concentrations higher than that used for drag reduction measurements.

A remaining issue in the practical application of polymer solutions is the gradual decrease of DR due to the scission of the long chain polymer molecules.[23] This is known as mechanical degradation and occurs under high shear conditions. It has ~~also~~ been observed that rigid polymers are more resistant to mechanical degradation than flexible polymers[8,24]. Soares et al.[25] argued that rigid polymers are not subject to the scission process, and the decrease in DR of rigid polymer, that is typically observed in the early stages of experiment, is associated with de-aggregation of polymer agglomerates. Vonlanthen et al.[26] developed a model for degradation of PEO based on a cascade in molecular weight distribution induced by the molecular scission. However, it is still challenging to model and predict the mechanical degradation of a drag-reducing polymer. In the current investigation, we will evaluate rheological properties to predict mechanical degradation of polymer solutions. The goal is to identify a rheological feature that can predict the resistance of polymer solutions to mechanical degradation.

Among the investigations of Table 1, only Owolabi et al.[19] observed a direct relationship between extensional viscosity and DR. However, this work was carried out only using PAM and oscillatory measurements were not conducted. In other investigations of Table 1, solution rheology was

characterized at concentrations higher than that used for DR tests. Another issue, that makes it difficult to propose a relation between DR and the non-Newtonian properties of the solution, arises from the fact that shear viscosity and viscoelasticity were simultaneously varied for the tested polymer solutions. This makes it more challenging to identify the primary parameters that correlate with DR. In the current investigation, we isolate the effect of shear viscosity to study the effects of extensional viscosity and viscoelasticity. This is carried out by adjusting the concentration of different rigid and flexible polymers, through trial and error, to obtain polymer solutions with the same shear viscosity at high shear rates. We chose to match the shear viscosities at high shear rates that are comparable to the shear rates experienced by polymer solutions in turbulent flows. Four solutions of flexible polymers (three of which are PAM and one PEO) along with two rigid polymer solutions (one XG and the other CMC) are chosen for the present investigation. The drag reduction of these polymer solutions , which have a common shear viscosity at high shear rates, are measured in a turbulent pipe flow. Their extensional viscosity and SAOS moduli are measured using CaBER and oscillatory tests at the same polymer concentration that was used for DR tests. The rate of mechanical degradation of the polymer solutions is also evaluated by monitoring pressure drop in the pipe loop over time. A direct comparison is made between the drag reduction efficiency of the pipe flow experiments and the viscoelastic properties discerned from the rheology measurements.

Table 1. A summary of the major investigations that have reported extensional viscosity and SAOS measurements of drag-reducing polymer solutions.

Source	Polymer type	Concentration for DR (ppm)	DR%	Oscillatory measurements	Concentration for oscillatory tests (ppm)	Extensional viscosity measurement	Concentration for extensional viscosity (ppm)
Escudier et al. (1999)	CMC, XG, PAA	2500-4000 2000 1250-2000	NA	No	NA	Yes	2500-4000 2000 1250-2000
Escudier et al. (2001)	XG, CMC	NA	NA	Yes	2500, 4000	No	NA
Nakken et al. (2001)	Poly α-olefin A	1-12	1-35	Yes	5000	No	NA
Japper-Jaafar et al. (2009)	Scleroglucan	750	47, 55	Yes	750, 5000	Yes	1000
Wyatt et al. (2010)	XG	60	11-16	Yes	60 (from 500 to 4000 ppm master solution)	No	NA
Pereira et al. (2012)	PEO, PAM	2-50	12-24, 2-20	Yes	10000	No	NA
Pereira et al. (2013)	PEO, PAM, XG	2-100	15-20, 7-21, 0.5-27	Yes	1000-10000 2500-10000 250-10000	Yes	1000-10000 2500-10000 100-10000
Owolabi et al. (2017)	PAA	250	72	No	NA	Yes	250
Present work	PAM, PEO, XG, CMC	20-170	10-58	Yes	20-170	Yes	20-170

II EXPERIMENTAL SETUP

The DR of the polymers was characterized through pressure drop measurement in a turbulent pipe loop. The preparation procedure of the polymer solution and measurement of shear viscosity, extensional viscosity, and storage and viscous modulus are detailed here.

A. Turbulent pipe flow

The DR measurements were conducted in a pipe with nominal diameter of D = 25.4 mm at a flow rate of 21.9 L/min. The schematic of the flow loop in Figure 1 shows the two pressure ports for measurement of pressure drop (ΔP), the reservoir, and the pump. The upstream pressure port is located at x = 1.5 m, where the origin of x is at the flange shown in Figure 1. This distance results in a flow development L/D = 59 to ensure a fully developed flow.[27] The downstream pressure port is at x = 2.5 m, which results in 0.032 ± 0.002 psi pressure drop between the two ports for flow of

water at Q = 21.9 L/min. A Validyne differential pressure transducer with 0.5 psi diaphragm was used for measuring the pressure drop. The signal was sampled at 2 Hz through a LabVIEW (National Instruments) interface.

One liter of high concentration polymer solution was produced by 2 hr mixing of polymer powder in distilled water using a magnetic stirrer as previously described by Mohammadtabar et al.[28] The concentrated solution was then gradually added to 70 L of distilled water in the mixing tank while the flow loop operated for 5 min to homogenously mix the polymer solution before the start of the data acquisition. A progressive cavity pump (Moyno, model 36704) and a variable frequency drive were used to circulate the flow. Flow rate was measured using a magnetic flow meter (Omega, FLR 8340D). The Reynolds number of the flow is $Re = U_b D/\upsilon$ = 20,600, where U_b, and υ are the bulk velocity and kinematic viscosity of water, respectively. The flow rate was kept constant during the experiments, which resulted in a constant U_b of 0.72 m/s for water and polymer solutions. A constant temperature of 25±0.5°C was also maintained. The *Re*, based on the viscosity of the polymer solutions at the wall shear rate (μ_w = 1.4 mPa.s), is 13,100. The pipes were completely washed after each polymer experiment, followed by pressure drop measurement with water to ensure no contamination from the previous test occurred. The wall shear stress is calculated using $\tau_w = \Delta P\ D/\ 4L$, where L =1 m is the distance between the pressure ports. The calculated wall shear stress for the Newtonian (water) flow is 1.4 Pa. Drag reduction percentage is estimated following[29]

$$DR\% = \left(1 - \frac{\Delta P_{polymer}}{\Delta P_{water}}\right) \times 100 \quad (1)$$

where ΔP_{water} and $\Delta P_{polymer}$ are the pressure drop measured for water and the polymer solution, respectively. In order to filter out the high-frequency fluctuations and investigate the mechanical degradation (variation of DR in time), a moving average with kernel of 250 seconds was applied to the pressure data recorded over a total duration of 2 hours. The mechanical degradation of the solutions is characterized as DR percent per time ($\Delta DR/\Delta t$, 1/min). The average pressure drop of the first 250 seconds is referred to as DR_0.

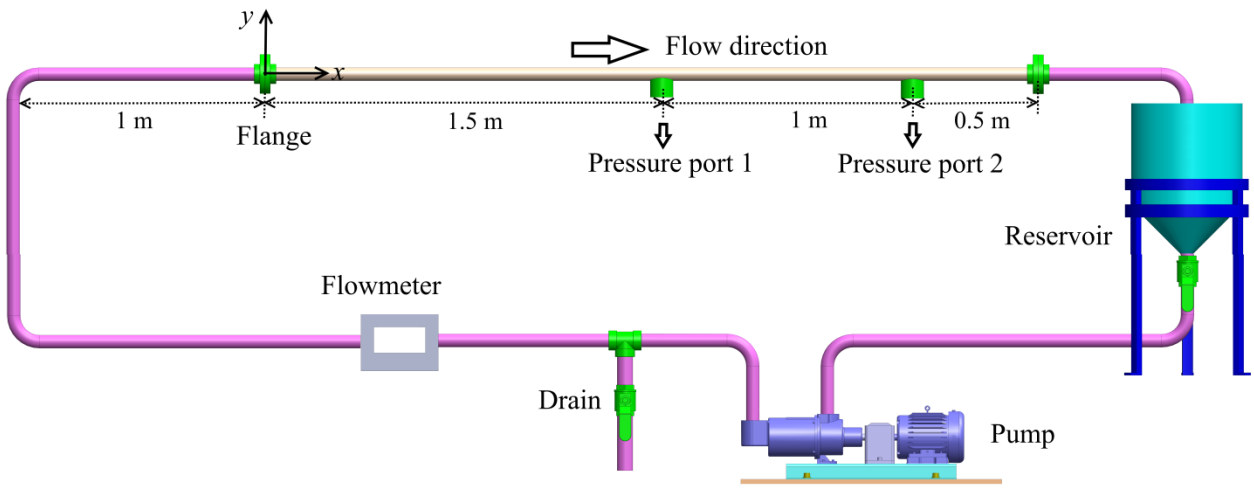

Figure 1. Schematic of the flow loop used for the drag reduction experiments.

B. Drag reducing polymers

Three flexible PAM polymers were used: Magnafloc 5250 (BASF Corp.), Superfloc A-110 (Kemira), and Superfloc A-150 (Kemira), and a PEO polymer (Sigma-Aldrich). These are high molecular weight anionic polymers (1×10^6 - 20×10^6 Da), which are used in mineral processing and tailings thickening.[30] Superfloc A-150 has a higher molecular weight and anionic charge relative to Superfloc A-110.[31] The PEO has a linear structure and a molecular weight of about 8 million Da.[32] Two rigid polymers with non-linear structures were selected for the current study: XG and CMC polymers. The molecular weight of XG is between 2×10^6 - 5×10^6 Da[33], and the molecular weight of CMC is between 90×10^3 to 700×10^3 Da[34]. The polymer type, structure, commercial name, manufacturer, and the abbreviation used to refer to each polymer are shown in Table 2.

Table 2. Polymers listed as part of the current study.

Polymer	Structure	Manufacturer	Commercial name	Abbreviation
Polyacrylamide	Flexible	Kemira	Superfloc A-150	SF-150
Polyacrylamide	Flexible	Kemira	Superfloc A-110	SF-110
Polyacrylamide	Flexible	BASF	Magnafloc 5250	MF
Polyethylene oxide	Flexible	Sigma-Aldrich	Polyethylene oxide	PEO
Xanthan gum	Rigid	-	Xanthan gum	XG
Carboxy methyl cellulose	Rigid	-	Carboxy methyl cellulose	CMC

C. Polymer rheology

For measurement of shear viscosity of the polymer solutions at high shear rates, a rheometer (RheolabQC, Anton Paar) with a double-gap Couette geometry (DG42) was used. The inner and outer radii of the measuring cup were 19.748 and 21.506 mm. The measuring bob also has a cylindrical geometry with inner and outer radii of 20.244 and 20.997 mm. Therefore, the inner and outer gaps of the double-gap Couette geometry were 0.496 and 0.510 mm, respectively. The effective length of the cylinders was also 78.700 mm. The small gap of this rheometer is suitable for viscosity measurements of low viscosity fluids at high shear rate. A water bath was used to maintain the temperature at 25±0.02˚C during the measurements. For the current polymer solutions, reliable measurements were obtained for shear rates between 160 to 710 1/s. The accuracy of viscosity measurements is estimated to be ± 2%.[35] For measurements of shear viscosity at low shear rates, we used a Discovery Hybrid Rheometer-2 (TA Instruments) with a concentric cylinder. The outer diameter of the inner cylinder was 28 mm and the inner diameter of the cup was 30.4. The cup length was also 30.4 mm. Using this geometry and instrument, we carried out shear viscosity measurements for a shear-rate range of approximately 1 to 100 1/s.

A HAAKE CaBER (Thermo Scientific) was used to measure the extensional viscosity of the polymer solutions. To make a measurement, a droplet of polymer solution was placed between two circular plates with 6 mm diameter and 3 mm distance. The top plate is suddenly lifted to stretch the polymer solution and form a filament. The final gap size is 9 mm with a strike time of 50 ms. The laser micrometer monitored the middle of the filament at a frequency of 10 kHz. The midpoint diameter of the filament (D_{mid}) was recorded using a laser micrometer as a function of time[36]. The elastic force is modeled using the upper-convected Maxwell model to correlate polymer stress with the deformation rate[37]. By fitting the data with $D_{mid}(t) = Ae^{-Bt} - Ct + E$, the relaxation time ($\lambda$) is estimated[38]. Here, $B = 1/3\lambda$. Hencky strain and strain rate are also calculated from the variation of D_{mid}. The apparent extensional viscosity, η_E, is estimated as [39]

$$\eta_E(\varepsilon) = -\frac{\sigma}{dD_{mid}/dt} \tag{2}$$

We also carried out measurements of surface tension (σ) using bubble pressure tensiometer (BO100, Krüss GmbH). The results shows that σ is approximately 73 mN/m for all the PAM solutions, while it is 63 mN/m for the PEO solution. Miller et al.[38] also reported σ of 73×10^{-3} N/m for a solution of 10,000 ppm PAM.

The viscoelasticity modulus is defined as $G^*=G'+iG''$, where G' and G'' are the elastic and viscous modulus, respectively. The oscillatory tests to determine G' and G'' were carried out using Discovery Hybrid Rheometer-2 (TA Instruments) with a concentric cylinder. Both amplitude and frequency sweep tests were conducted. The minimum measurable torque using this rheometer was 0.002 μN.m. The measured torque in the current study varied from 0.1 μN.m to 640 μN.m. In the amplitude sweep tests, a fixed angular frequency (0.628 rad/s) was used while stress was slowly increased from 0.00085 to 0.0673 Pa. In the frequency sweep tests, a fixed oscillation displacement of 0.1 rad was applied and the angular frequency was varied from 0.628 to 18.84 rad/s. All rheological characterizations were carried out with a fresh solution, prior to the drag reduction tests (no mechanical degradation). The measurements were also repeated five times to estimate the measurement uncertainty.

III. RESULTS

In this section, we first select a reference polymer solution based on the DR performance of SF-150. The viscosity of this solution at high shear rates determines the target value to which the other flexible and rigid polymer solutions will be tested at. Secondly, we measure DR and the extent of mechanical degradation for each of the polymer solutions. Finally, the extensional viscosity and SAOS properties of the solutions are investigated to evaluate their relationship with DR and mechanical degradation. As it was indicated in Table 2, we will use four flexible polymers (SF-150, SF-110, MF, PEO), and two rigid polymers (XG and CMC). Three of the flexible polymers (SF-150, SF-110, and MF) are polyacrylamides (PAM).

A. Determination of the reference shear viscosity

Drag reduction of SF-150 solutions at 20, 30, 40, and 50 ppm is shown in Figure 2. The 20 ppm tests are repeated twice to provide an indication of the process uncertainty. The discrepancy of the two tests is about 2% over the 2 hours of measurement. This error can originate from uncertainties in polymer preparation, pressure measurement, and flow rate. It is observed that at 20 ppm, an initial DR of 58% is obtained. After 2 hours of flow circulation in the loop, the high shear in the pump degrades the polymer and reduces the DR to 37%. The drag reduction at 30 ppm also starts at 60%, similar to the 20 ppm solution. However, the pump shear results in a smaller degradation of the 30 ppm solution. The mechanical degradation at 40 ppm is negligible and DR remains about 60-62% during the measurement period. The slight increase of DR is associated with experimental

uncertainties and further mixing of the solution within the flow loop. Drag reduction at 50 ppm is smaller, potentially due to its higher shear. Since we intend to study degradation, SF-150 at 20 ppm was selected as the reference flexible polymer. This solution is more prone to degradation than the higher concentration SF-150 solutions. In addition, the solution of 20 ppm SF-150 has a relatively small shear viscosity, which can be achieved using polymers with a lower MW. For example, a large concentration of PEO is needed to reach the same high-shear viscosity as SF-150.

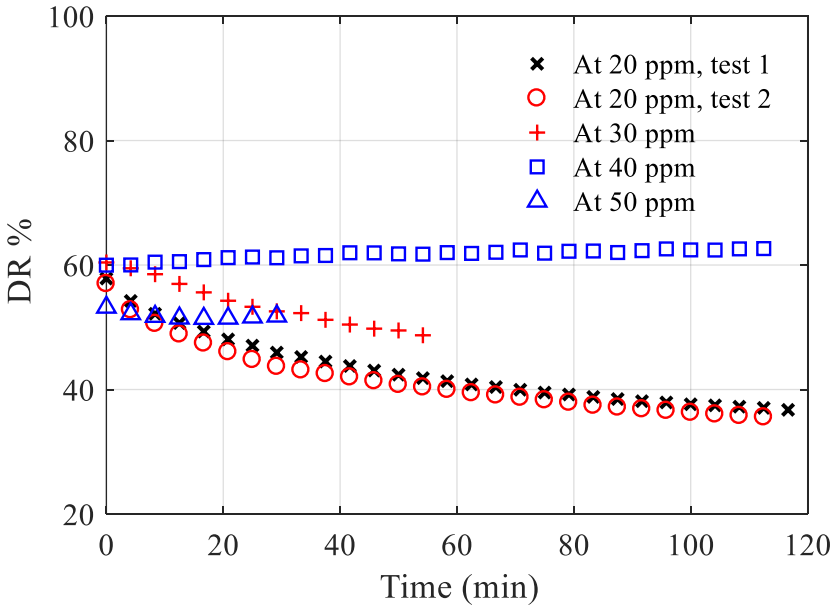

Figure 2. Drag reduction of SF-150 polymer solutions tested at different concentrations. The test at 20 ppm is repeated to evaluate the uncertainty of the polymer mixing procedure and pressure drop measurements.

The viscosity of the reference polymer solution (20 ppm of SF-150) at high shear rates was measured using the double-gap rheometer. Then, the concentrations of the other polymer solutions were varied by trial and error to produce the same high-shear viscosity. This procedure for MF and PEO is illustrated in Figure 3, which shows shear viscosity measurements of MF solutions (22, 26, and 28 ppm), and PEO solutions (50, 100, 170, 185, and 200 ppm) for shear rates between 160 to 710 1/s. Comparison of Figure 3(a) and (b) shows that a larger change in concentration of PEO is required with respect to MF to result in a similar change in shear viscosity. This is attributed to the larger MW of MF. Similar trial and error experiments have been carried out for the other polymers to obtain the concentration required to produce the same shear viscosity as the reference case at high shear rates (160 to 710 1/s). The high-shear viscosity of each polymer solution at the final concentration is demonstrated in Figure 4(a). As it is observed, all the viscosities approximately

overlap and approach a common value of 1.4 mPa.s with increasing shear rate. It can be observed that the measured shear viscosities are within 5% of the reference SF-150 solution. These selected concentrations are used to investigate DR, mechanical degradation, and the solution rheology in the next sections. The matching viscosity is obtained here at high shear rates that are typically observed in turbulent flows. For example, Shaban et al.[40] showed that in a turbulent channel flow at Re = 20000, the maximum instantaneous shear rate can exceed 1000 1/s while the mean shear rate is approximately 400 1/s.

To characterize the viscosity of the polymer solutions at low shear rates, additional measurements were carried out using the Discovery Hybrid Rheometer-2 equipped with a concentric cylinder. As it is shown in Figure 4(b), the shear viscosities of the polymer solutions do not match at shear rates smaller than 100 1/s. Except PEO, all the polymer solutions exhibit a shear thinning behavior. The PAM solutions (SF-150, MF, SF-110) have a strong shear thinning trend while the rigid polymers (XG and CMC) show a mild shear thinning trend. However, with increasing shear rate, the viscosities approach a common high-shear viscosity. Therefore, the shear viscosity of the polymer solutions is only matched for share rates larger than 100 1/s.

(a)

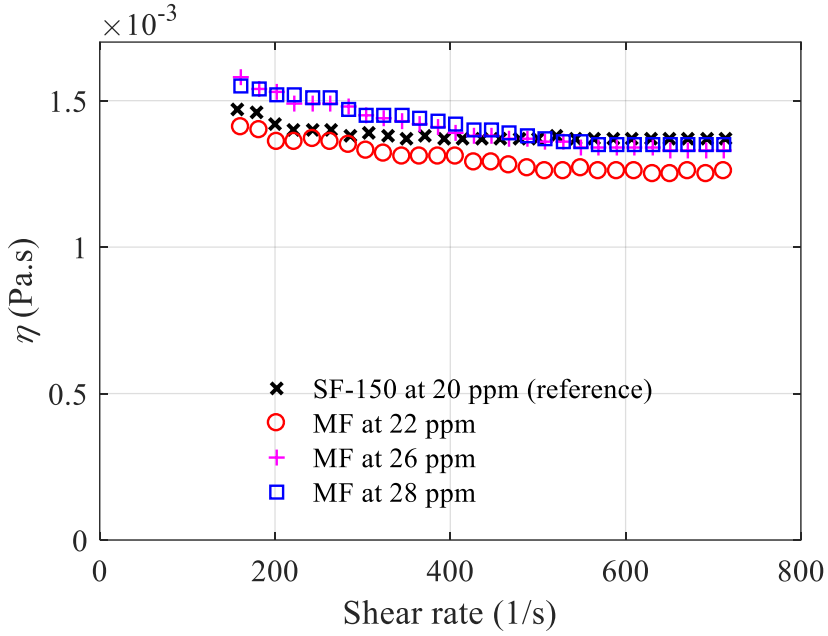

(b)

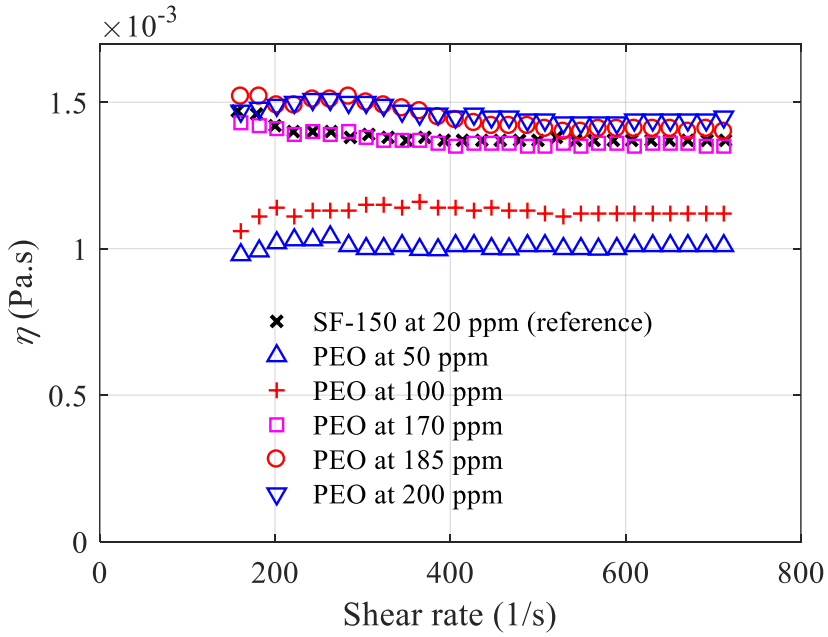

Figure 3. Variation in shear viscosity of (a) MF and (b) PEO solutions with concentration. The shear viscosity of the reference 20 ppm SF-150 solution at is also shown for comparison.

(a)

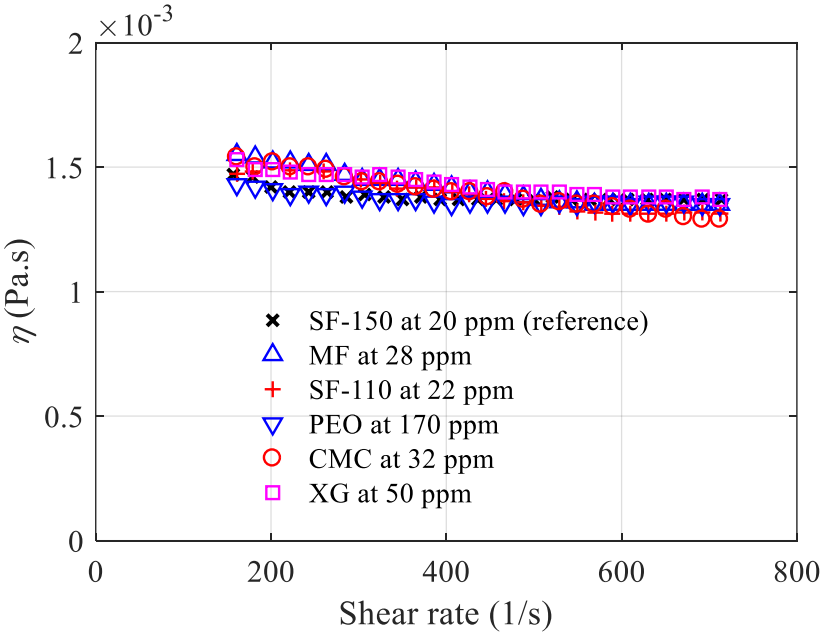

(b)

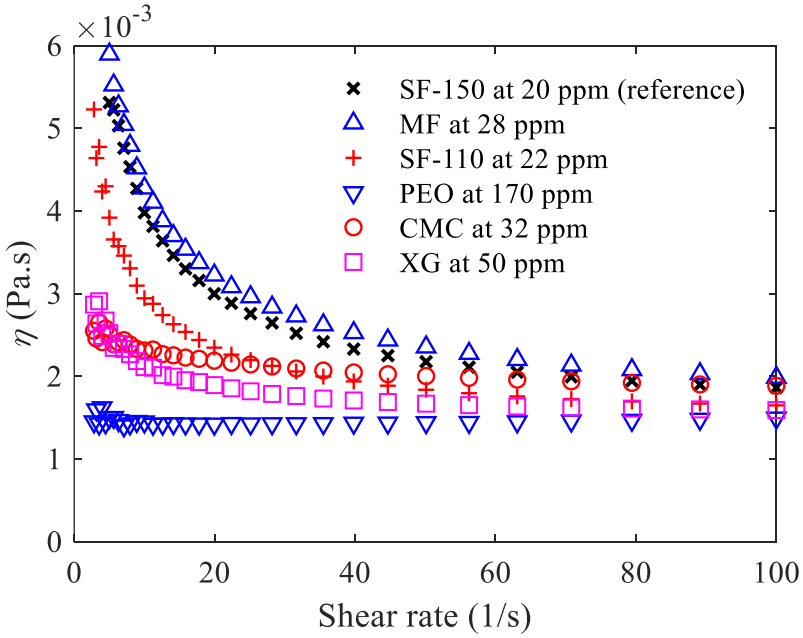

Figure 4. The shear viscosity of the polymer solutions at the selected concentrations for (a) high shear rates of 160 to 710 1/s and (b) low shear rates of approximately 1 to 100 1/s. In the high shear range, the maximum difference in shear viscosity between the reference polymer and the other polymer solutions is 5%, occurring at shear rate of ~200 1/s.

The selected polymer concentrations are smaller than the overlap concentration (c^*) reported in the literature for PEO, XG, and CMC solutions. Escudier et al.[41] obtained c^* of 670 ppm for XG

and 300 ppm for polyacrylamide solutions. Thus, polyacrylamide solutions (20-28 ppm) and XG (50 ppm) solutions used in this study can be considered dilute. Dinic et al.[42] also estimated c^* of 1700 ppm for the PEO solution, which is larger than the 170 ppm concentration of PEO used in this study. Therefore the 170 ppm solution of PEO is dilute as well.

B. Drag reduction and mechanical degradation

The DR of each polymer solution, measured over 2 hours, is shown in Figure 5. For all the polymers, maximum value of DR is found at the beginning of the test, followed by a gradual reduction due to mechanical degradation. The initial DR of PEO is the lowest among the flexible polymers (DR_0 = 44%) and its DR capability disappears after 25 min. The SF-150 has the highest DR up to 45 min, when degradation reduces its DR slightly below that of MF, showing slightly more susceptibility to mechanical degradation relative than MF. Drag reduction of both SF-150 and MF is greater than that of SF-110. Mechanical degradation of SF-110 and SF-150 solutions follows similar trends. DR of XG and CMC demonstrate negligible degradation, and are both approximately equal to 10%. The mechanical degradation of the solutions, characterized as percent of DR per time ($\Delta DR/\Delta t$, 1/min), is estimated over the measurement time and shown in Table 3. The results show that the flexible polymers have the largest initial DR_0 of 50-58% with a degradation rate of 0.12-0.17 1/min. PEO has DR_0 of 44% while its degradation rate is significant at about 1.74 1/min. The rigid polymers have a small DR of 10-12% with negligible degradation of 0.01 to 0.03 1/min. Therefore, we observe that solutions of different flexible and rigid polymer, but a similar high-shear-rate viscosity, demonstrate different DR and mechanical degradation rates. This observation proves that DR and mechanical degradation of the solutions are independent of their shear viscosity at high shear rate.

As it was mentioned in Section II.A, the polymer solution was circulated for 5 min in the flow loop before the start of data acquisition. During this 5 min, the DR performance of the polymers that are highly susceptible to degradation, such as PEO, can considerably change. Therefore, we use a second-order polynomial to extrapolate the DR to 5 min prior to the start of data acquisition. The extrapolated value is indicated by DR'_0 in Table 3. The polynomial is also visualized by dashed lines in Figure 5. The estimated DR'_0 does not include the effect of degradation, and will be used to investigate the correlation of drag reduction with solutions rheology.

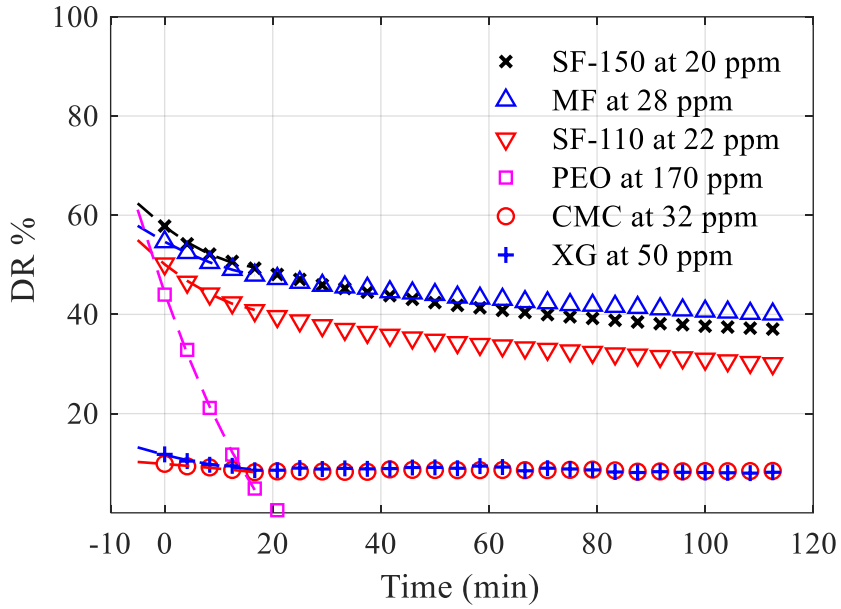

Figure 5. Drag reduction of flexible and rigid polymer solutions as the solution circulates in the flow loop. All polymer solutions have the same shear viscosity (see Figure 4). The dashed lines shows the second order polynomial used to extrapolate the data to 5 min prior to the start of data acquisition.

C. Extensional viscosity

The variation in filament diameter as a function of time, obtained from CaBER measurements, is demonstrated in Figure 6. The reference time of $t = 0$ indicates when the top plate reaches the final 9 mm gap and stops. The filament of the XG and CMC (rigid polymers) broke at about $t = 0$, and therefore, are not shown in Figure 6. The rapid rupture of the filaments for these polymers indicates that they have a negligible extensional viscosity. At $0 < t < 0.08$ s, SF-150 and PEO have the thickest and the thinnest filaments, respectively. MF has a thicker filament dimeter relative to SF-110. The break up time for SF-150 and SF-110 are 0.11 and 0.07 s while it is 0.08 s for MF. PEO maintains the thinnest filament that stretches up to 0.5 s (not shown here).

An exponential decay of filament diameter should appear linear in the semi-logarithmic plot of Figure 6(a). Therefore, the relaxation time of the polymer solutions is calculated by fitting $D_{mid}(t) = Ae^{-Bt} - Ct + E$ on the linear section of the data in Figure 6(a). The data range that is used to fit the function is iteratively selected to limit the maximum deviation to 5%. The magnitude of the estimated relaxation times is shown in Table 3. The results show that PEO has the largest relaxation time, followed by SF-150, MF, and SF-110. The relaxation time of the rigid polymers (XG and CMC) is negligible and not measurable using the CaBER system as the filament quickly ruptured.

The high relaxation time of SF-150, MF, and SF-110 is correlated with their larger DR_0 and DR'_0 values as shown in Table 3. However, for PEO, the correlation is only observed between DR'_0 and high λ. PEO has the lowest DR_0 of 44% among the flexible polymer solutions while it has the largest value of λ. The discrepancy is associated with the high degradation rate of PEO ($\Delta DR/\Delta t$ = 1.74 1/min); an initially high DR of PEO has quickly degraded within the first five minutes of circulating the solution in the loop, before the start of the data acquisition. The extrapolation of PEO data in Figure 5 to 5 min before the start of data acquisition results in DR'_0 of 61%, which would be consistent with its higher λ. The smaller DR of XG and CMC polymers also agrees with their negligible λ.

The Weissenberg number can be calculated as $Wi = \lambda\, d\langle U\rangle/dy$, where $\langle U\rangle$ is the mean velocity of the turbulent pipe flow and $d\langle U\rangle/dy$ is the shear rate of the mean flow at the wall. The wall shear rate is obtained from $d\langle U\rangle/dy = \tau_w / \mu_w$, where μ_w is the shear viscosity of the polymer solution at the mean shear rate of the fluid at the wall. As mentioned earlier, τ_w is determined from pressure drop measurements within first 5 minutes of data acquisition. The viscosity at the wall (μ_w) is estimated from shear viscosity measurements of Figure 4, and is approximately 1.4 mPa.s for shear rate varying from 400-700 1/s. The estimated magnitude of $d\langle U\rangle/dy$ and Wi for the flexible polymer solutions is presented in Table 3. An inverse relationship between DR'_0 and the mean velocity gradient at the wall is observed here: the larger the DR'_0, the smaller is the value of $d\langle U\rangle/dy$. As Table 3 shows, Wi of PEO is larger relative to that of the other flexible polymers while Wi of XG and CMC should be negligible. Therefore, similar to the previous discussion of the relationship between λ and DR'_0, large Wi indicates large DR'_0.

To further investigate the filament decay, the decay of the filament diameter is shown in linear axes in Figure 6(b). We observe that filament decay is initially linear at -0.03s < t < -0.01s following a Newtonian response of $D_{mid} \propto -t$.[43] Beyond this linear regime, decay of the filament reduces, and filament diameter gradually reduces. As we observed in Figure 6(a), in this region the decay is exponential, indicating viscoelastic behavior of the fluid.[44] For the PAM filaments in Figure 6(b), the viscoelastic stretching starts earlier at about t=-0.015s, then the filament gradually decays and ruptures. However, for PEO, the filament follows a linear decay up to t = 0. Then, it suddenly transitions into a very slow decay that lasts for up to 0.5s (not shown in Figure 6).

Therefore, the viscoelastic behavior of PEO filament starts later (further stretched) with respect to the PAM filaments.

(a)

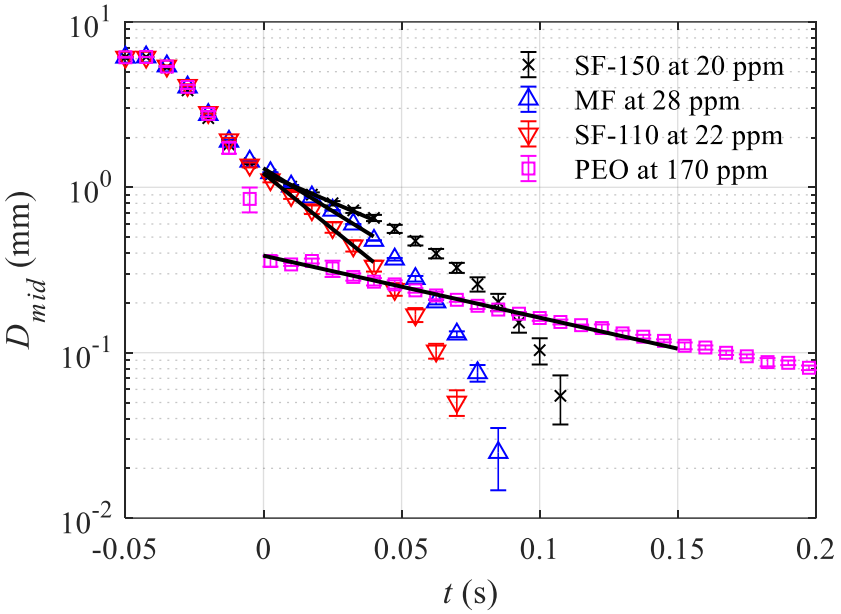

(b)

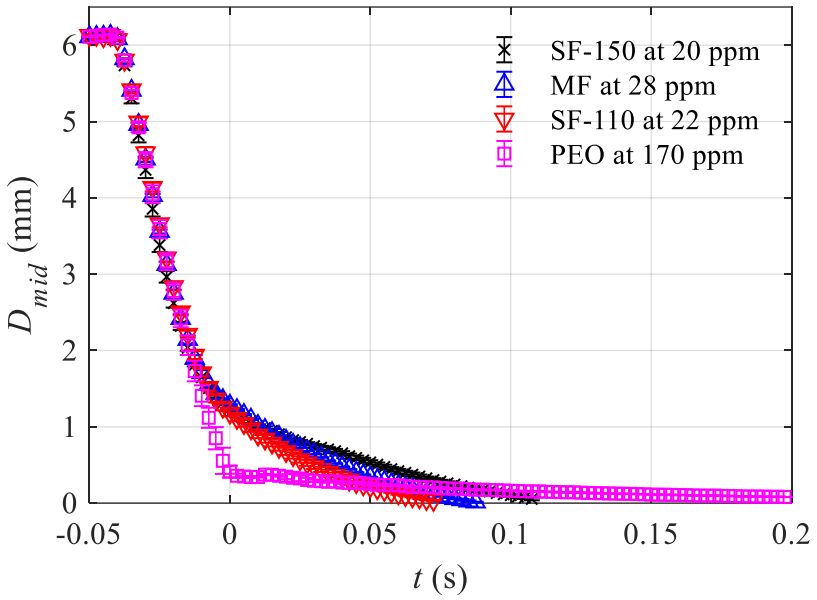

Figure 6. Measurement of the filament diameter of the polymer solutions using CaBER in (a) semi-logarithmic and (b) linear axes. For clarity of the plot, the temporal resolution is down-sampled by a factor of 75; only one out of every 75 data points is presented in time. The error bars represent the standard deviation of filament diameters based on five measurements.

Table 3. Relaxation time, wall shear rate, Weissenberg number, DR_0 (at $t = 0$), $\Delta DR/\Delta t$ for flexible and rigid polymer solutions. All polymer solutions have the same shear viscosity.

Polymer solutions	DR_0	DR'_0	$\Delta DR/\Delta t$ (1/min)	λ (ms)	Wall shear rate (1/s)	Weissenberg number (Wi)
SF-150	58	62	0.17	20	407	8
MF	55	58	0.12	14	448	6
SF-110	50	55	0.17	11	486	5
PEO	44	61	1.74	40	528	21
XG	12	13	0.03	~0	896	~0
CMC	10	10	0.01	~0	915	~0

The dependency of DR with *Wi* number was evaluated by Owolabi et al.[19]. They used two types of PAM solutions: FloPAM at three concentrations (150, 250, and 350 ppm) and Separan at 250 ppm and they measured DR in a pipe, a rectangular channel, and a square duct. They proposed an empirical equation to predict DR as a function of *Wi* and a critical Weissenberg, $Wi_c = 0.5$, which indicates the onset of DR. This equation shows increase of DR when *Wi* increases up to 6. Beyond $Wi = 6$, an asymptotic behavior at DR of 64% is observed, where DR becomes independent of *Wi*. An estimation of DR, based on the Owolabi et al.[19] model, shows that this model overestimates DR of SF-150, MF, and SF-110 by 10, 17, and 27% with respect to the measurements. It should be noted that the uncertainty of Owolabi et al.[19] appears to be about ±8%; some of their experimental results for $Wi \sim 5$ fall in the range of 59-75% DR. Another reason for the discrepancy is the mechanical degradation of the polymer solutions within the first 5 min of flow circulation before data acquisition and during the data acquisition process. This changes their λ and *Wi* values. Nevertheless, the evaluation suggests correlation of DR with both λ and *Wi*. Comparison of polymers ability for DR based on λ can be straightforward since it only requires CaBER measurements. However, the measurements in Table 3 do not show any relation between mechanical degradation of the polymer solutions and their relaxation time.

The extensional viscosity for the solutions of flexible polymers is presented as a function of strain and strain rate in Figure 7(a) and (b), respectively. The direction of increasing time (t), and the moment when the CaBER endplate stops ($t = 0$) are also shown in these figure. In Figure 7(a), during the endplate stroke ($t < 0$), η_E gradually increases to about 0.01 Pa.s for all the polymer solutions. However, after the stroke ($t > 0$), PEO filament undergoes significantly larger strain within two different straining regimes. First, a rapid increase of η_E over a small range of strain. In this regime, η_E of PEO rapidly increases to 0.25 Pa.s with a small increase of strain. For the PAM

filaments, η_E increase to about 0.05 Pa.s while the filaments are subject to a larger strain increment. In the second region, a slower increase of η_E is observed. The increase of η_E is again larger for PEO and η_E exceeds 1 Pa.s.

The variation of η_E with strain rate in Figure 7(b) shows an initial increase of extensional viscosity with increasing strain rate for $\eta_E < 0.01$ Pa.s. White et al.[45] described this behavior as a Newtonian response for an extensional rate that is lower than the onset of extensional thickening. Then at $t = 0$, there is a sharp transition to extensional thickening where strain rate decreases with increasing η_E. These two regions are present for all the filaments. For the PEO filament, the regions extend to larger strain rates and η_E. At the end of the extensional thickening, a Newtonian regime is observed again for all the PAM filament; η_E increases with increasing strain rate. However, the PEO filament shows a region where η_E rapidly increases while the strain rate slightly decreases. Therefore, PEO has a different trend in which extensional shear thickening occurs from $t = 0$ until the breakup point.

(a)

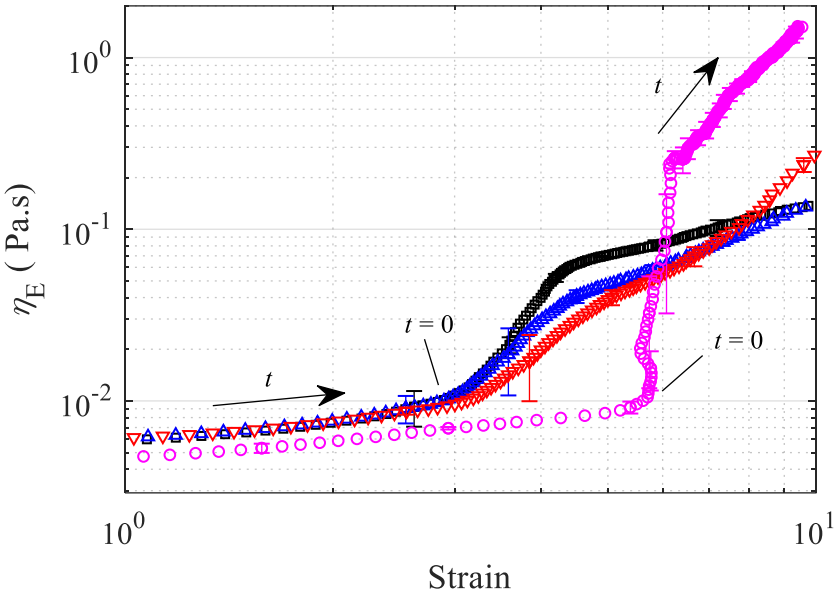

(b)

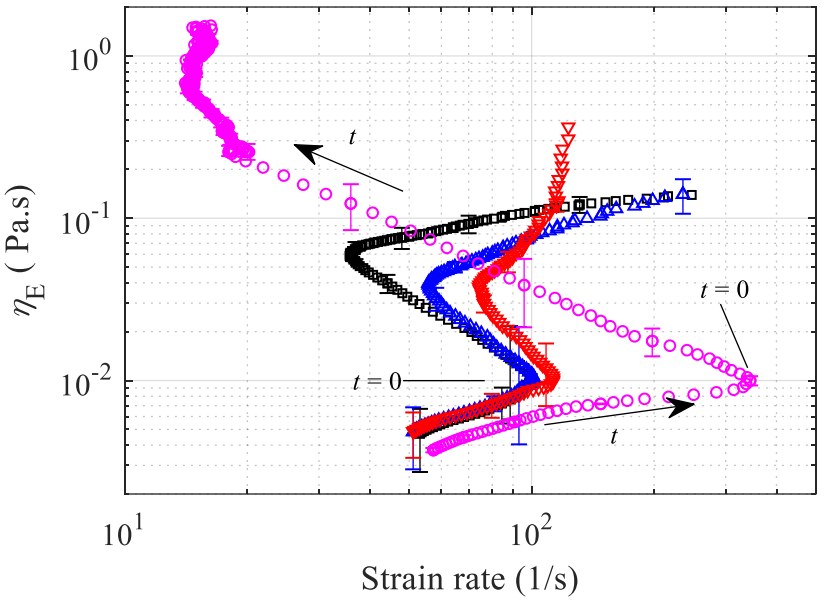

Figure 7. Variation of extensional viscosity with (a) strain and (b) strain rate for the flexible polymer solutions. Only one out of 50 data points is presented for the clarity of the plot. The error bars represent the standard deviation of the values based on five measurements.

D. Oscillatory rheology

The SAOS measurements at a constant angular frequency of 0.628 rad/s are shown in Figure 8. The results show storage modulus (G'), loss modulus (G''), and their ratio (G'/G''). The ratio G'/G'' indicates whether the solution dissipates ($G'/G'' < 1$) or temporarily stores ($G'/G'' > 1$) the turbulent

kinetic energy. To evaluate the random noise, the measurements are repeated 5 times and the standard deviation of measurements is calculated and shown using the error bars. In addition, to evaluate the bias errors, Figures 8 also shows oscillatory measurements for water. It is observed in Figure 8(a) that, for stress values smaller than 0.03 Pa, G' of the polymer solutions is an order of magnitude larger than that of water. This indicates the validity of the measurement in this region. For stress values larger than 0.03 Pa, G' for water and some of the polymer solutions have a similar magnitude, showing a large uncertainty at high stress values. Therefore, only the measurements for stress values smaller than 0.03 Pa are reliable in Figure 8(a). Figure 8(b) shows that polymer solutions have greater G'' compared with water over the entire range of strain rates.

In Figure 8(a) and (b), a region of constant G' and G'' is observed for all the polymer solutions at stress values smaller than 0.01 Pa. The constant values of G' and G'' at the small stress values indicate a linear viscoelastic region (LVR), which is followed by a gradual decrease of G' and G'' in the non-linear region. The reduction of G' and G'' is an indication of strain thinning behavior in large-amplitude oscillatory shear (LAOS). Townsend and Wilson[46] associated this behavior to untangling and aligning of polymer chains with the flow at high oscillating amplitudes (i.e. stress). The PAM solutions (SF-110, SF-150, and MF) have the largest values of G' and G'', while PEO has the smallest values. The G' and G'' of the rigid polymers (XG and CMC) fall between the PAM and PEO solutions.

The larger G' modulus of the PAM solutions indicates that they can store turbulence kinetic energy. This observation supports the mechanism proposed by De Gennes[15] and agrees with the greater DR capability of PAM polymers. The larger G'/G'' ratio for SF-150, SF-110, and MF solutions in Figure 8(c) also shows their higher elasticity with respect to the other polymer solutions, which is correlated with their better DR performance. The smaller G' of the rigid polymers is in agreement with their smaller DR. The G'/G'' ratio of CMC and XG solutions is small in Figure 8(c), which indicates greater viscous dissipation than elastic behavior. This is expected since a large viscous dissipation (small G'/G'') converts turbulent kinetic energy into heat and is not desirable for DR. However, the small G' and G'/G'' of PEO are not correlated with its relatively high DR. Except for PEO, solutions with large G' and G'/G'' result in a high DR.

The measured G' and G'' from the frequency sweep tests at a fixed oscillation displacement of 0.1 rad are shown in Figure 9. To evaluate the measurement uncertainty, Figure 9 also shows the

measured G' and G'' for water. For a Newtonian fluid, $G' = 0$ and $G'' = \mu\omega$, where μ is the dynamic shear viscosity and ω is the rotor displacement frequency. In Figure 9(a), G' for water increases with increasing angular frequency. This indicates the maximum bias error of the measurement that also increases with ω. The latter error is due to the larger inertial effects of the measuring bob (rotating cylinder) and the fluid at higher ω. Nevertheless, the measurements are valid at small ω, since G' of the polymer solutions is several times larger than G' of water. With increasing ω, the difference between G' for polymer solutions and water decreases and the magnitudes approach the same value at about ω=10 rad/s. If at least a twofold difference between G' of water and polymers is desirable, a cut-off of $\omega < 3$ rad/s should be considered for investigating Figure 9(a). In Figure 9(b), the theoretical G'' for water is shown by the dash line. A good agreement between the theoretical and measured G'' of water is observed at $\omega < 3$ rad/s. Again, uncertainty increases with increasing angular frequency, and the data for $\omega > 3$ rad/s should not be considered. It is important to note that the uncertainties are present here since the solutions are dilute and have a lower viscosity.

It is observed that G' and G'' of all polymer solutions increase with increasing ω. This trend indicates stronger viscoelastic behavior at higher angular frequencies. Escudier et al.[21] measured G' and G'' for 2500 ppm XG solution and 4000 ppm CMC solution in the frequency range of 0.007-70 rad/s. With increasing frequency, they observed that G' and G'' of XG increased from 0.01 to 5 Pa and from 0.05 to 4 Pa, respectively. The G' and G'' of CMC also increased from 0.0008 to 5 Pa and from 0.003 to 7 Pa, respectively. In Figures 9(a) and (b), the PAM polymers have the largest G' and G'', PEO has the smallest moduli across all the angular frequencies, while those of rigid XG and CMC polymers fall between PEO and PAM polymer solutions. The larger G' modulus for PAM polymers is in agreement with their larger DR. The trend of G'/G'' observed in Figure 9(c) is similar to Figure 8(c). The PAM solutions have larger G'/G'' ratios than the rigid polymers, which results in stronger elastic behavior and higher DR. Again, PEO solution appears as an anomaly. As seen in figure 9(c), for most of the polymer solutions, G'/G'' is slightly smaller than one, indicating that viscous effects are stronger than the elastic behavior in the linear viscoelastic limit.

(a)

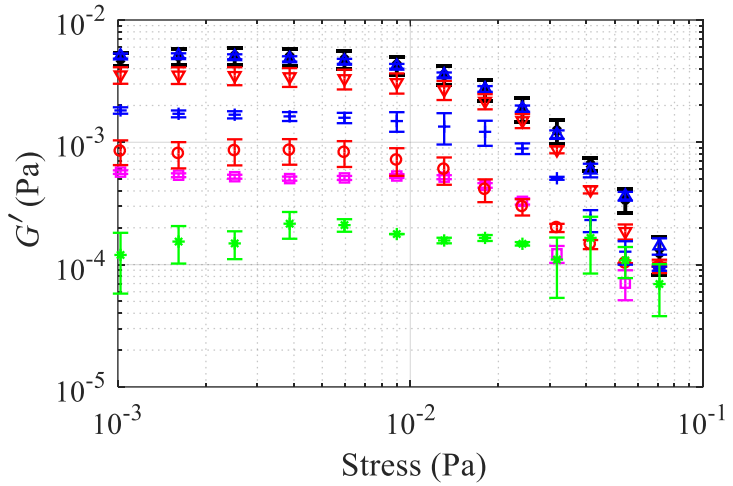

(b)

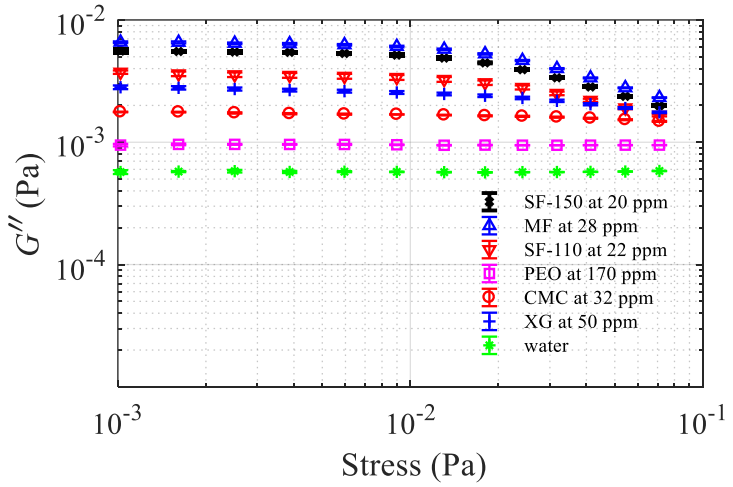

(c)

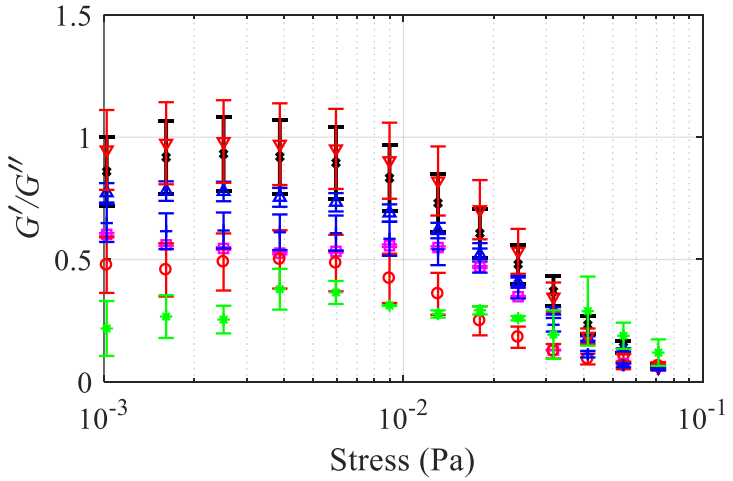

Figure 8. (a) Storage modulus, (b) loss modulus, (c) the ratio of storage to loss modulus for polymer solutions as a function of strain rate during a stress sweep test with constant oscillation angular frequency of 0.628 rad/s The error bars represent the variation of *G′, G″, and G′/G″* based on five independent measurements.

(a)

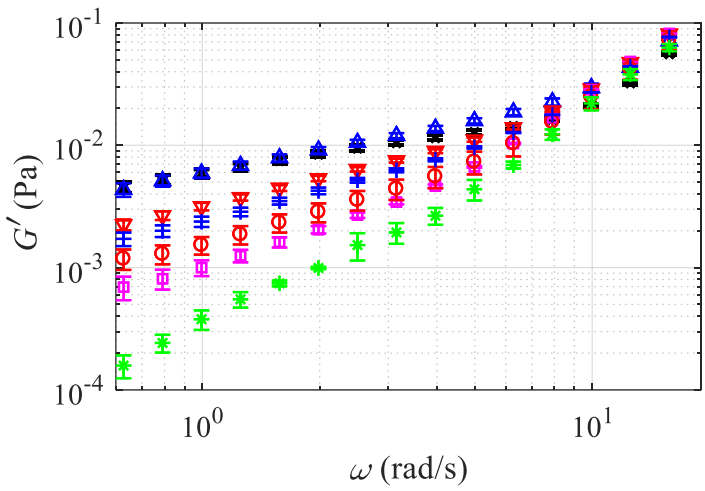

(b)

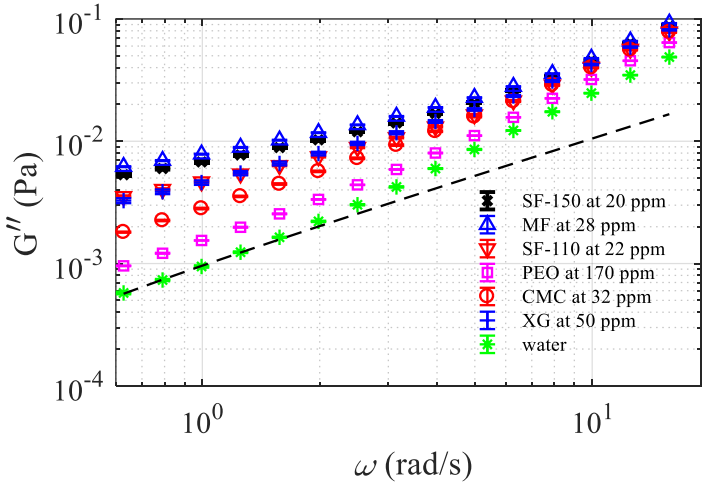

(c)

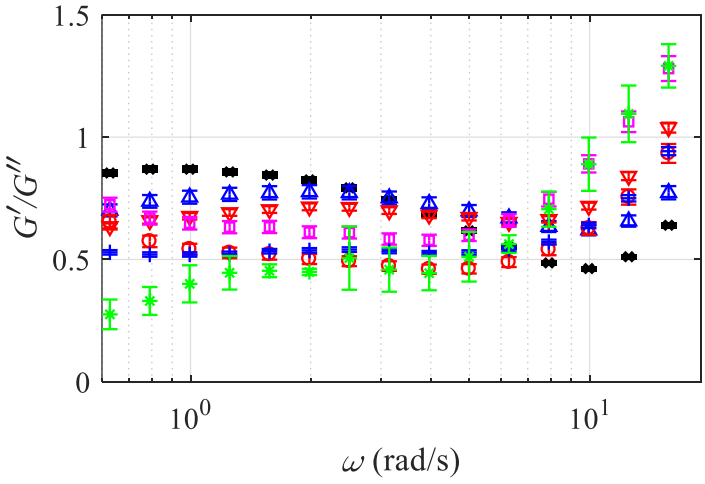

Figure 9. (a) Storage modulus, (b) loss modulus, (c) the ratio of storage to loss modulus for polymer solutions as a function of strain rate during a frequency sweep test with oscillation displacement of 0.1 rad. The error bars represent the variation of *G′,G″, and G′/G″* based on five measurements. The dashed line in Figure 9(b) shows theoretical results for water solution.

IV. DISCUSSION

The investigations characterized the DR performance and viscoelastic properties of several flexible and rigid polymer solutions. To simplify the analysis, the polymer concentrations were adjusted to match the shear viscosity of the solutions at high shear rates that are comparable with the shear rates typically observed in turbulent flows (larger than 100 1/s). The results showed that for solutions with similar high-shear-rate viscosity, DR widely varies from a negligible value up to large DR percent; flexible polymers (SF-150, MF, SF-110, and PEO) demonstrated large DR (more than 50%) while the rigid polymers (XG and CNC) demonstrated a smaller DR (approximately 10%). At shear rates smaller than 100 1/s, the polymers demonstrated a shear thinning behavior, with the exception of PEO. The PEO solution demonstrated no shear thinning while it resulted in a large DR. This anomaly indicates that polymer drag reduction is not correlated with the shear thinning behavior that is typically observed in steady shear rheometry of polymer solutions.

To characterize the viscoelastic properties, we conducted both SAOS and extensional rheometry. Although both measurements characterize viscoelasticity of the solutions, SAOS correspond to a "weak" flow and the extensional rheometer corresponds to a "strong" flow[47]. The weak versus strong flow classification is based on the degree of extension and alignment of the polymers with the principal axes of stretching. In SAOS measurements, the polymer molecules tumble due to the vorticity field and are not subject to full stretching. In filament stretching rheometry, the filament is irrotational and the polymer molecules can be fully stretched[47]. Therefore, the state of the polymer molecules and the viscoelastic properties that are obtained from SAOS and filament stretching can be different.

To further investigate the relation between DR and SAOS, Figure 10(a) and (b) show the relation of DR'_0 with G'/G'' at constant ω and at constant oscillation amplitude, respectively. In Figure 10(a), G'/G'' is averaged over 0.001 to 0.01 Pa (LVR range), and in Figure 10(b) G'/G'' is averaged over 0.6 to 3 rad/s. In both cases, G'/G'' is smaller than one; viscous behavior dominates elastic behaviour. In Figure 10(a), DR'_0 does not demonstrate any specific trend with respect to G'/G''. For example, G'/G'' of PEO with large DR'_0 is smaller than XG with a smaller DR'_0. In Figure 10(b), there is a rough trend of increasing DR'_0 with increasing G'/G''. However, the discrepancy with respect to the linear fit is large and a correlation is not trivial. Therefore, for a constant

oscillation frequency, SAOS does not correlate with DR of the polymer solutions, while a stronger correlation is observed between SAOS and DR when oscillation displacement is kept constant.

The relation of DR'_0 with extensional rheology of the solutions is investigated in Figure 10(c) using *Wi*. The trends shows an initial rapid increase of DR'_0 with increasing *Wi* up to approximately *Wi* = 5, followed by a plateau in DR'_0. The results show a correlation between DR'_0 and *Wi*, which agrees with the model suggested by Owolabi et al.[19] for PAM polymers (shown by the dashed line). We should note that the extensional viscosity and *Wi* of the rigid polymer solutions is zero here. Therefore, further investigation of the relation between DR and extensional rheometry of rigid polymer solutions at higher concentration (and DR) is needed to verify the Owolabi et al.[19].

The above observation indicated that the fluid properties obtained from the linear SAOS could not predict the drag reduction of the polymer solutions. This is consistent with the fact that a turbulent flow consists of motions with large amplitude and frequency of strain. Such a flow does not follow the flow condition of linear rheology. The strain amplitude and frequency within a turbulent flow are beyond the limits of SAOS measurement in Figure 8 and 9. Therefore, the results hint using LAOS for characterization of viscoelastic properties of drag-reducing polymer solutions. LAOS is suitable for characterization of non-linear viscoelasticity and the transient response of the fluid, as it is present in turbulent flows.[48]

The rheological properties of the polymer solutions were also evaluated for predicting the mechanical degradation of the polymer solutions. The mechanical degradation of PEO was an order of magnitude larger than the PAM polymers, while the rigid polymers demonstrated negligible mechanical degradation. The larger degradation of PEO is related to its unique variation of extensional viscosity with strain rate. The CaBER measurements showed that PEO has an extensional thickening behavior (i.e., increase of extensional viscosity with decreasing strain rate) that continues until the filament breaks up (see $t > 0$ in Figure 7(b)). In contrast, PAM solutions have a shorter extensional thickening region which is followed by a Newtonian behavior (i.e., increase of extensional viscosity with increasing strain rate) prior to the filament break up. The continuous extensional thickening behavior of PEO filament can be the reason for its faster mechanical degradation. Since strain rate decreases during the PEO filament drainage, it is hypothesized that the PEO molecules resist the stretching process more than PAM. This results in an excessive increase of extensional viscosity and scission of the filaments. In contrast, PAM

filaments accommodate the stretching process by allowing for an increase of strain rate, which relaxes the increase of extensional viscosity.

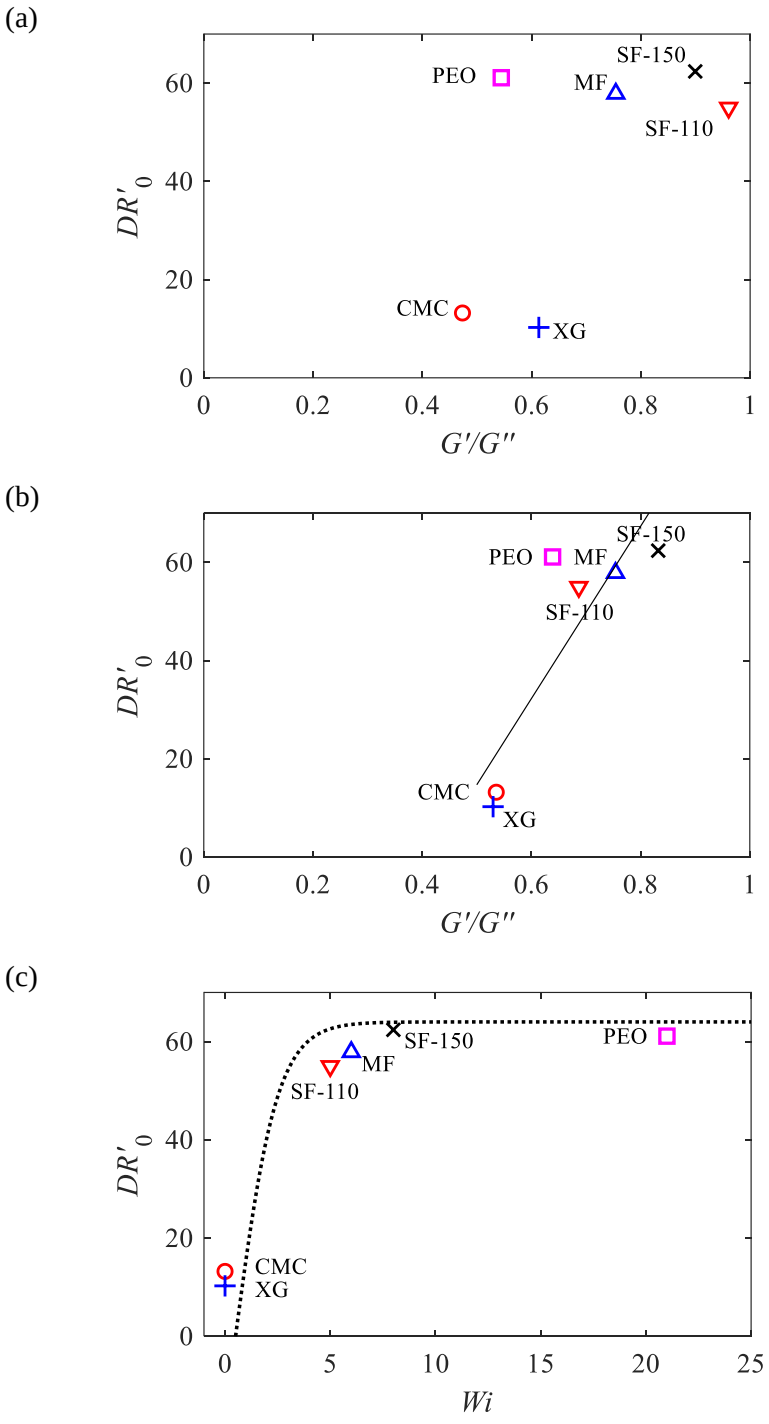

Figure 10. Variation of DR'_0 with (a) G'/G'' averaged over 0.001 to 0.01 Pa for a constant oscillation frequency of 0.628 rad/s, (b) G'/G'' averaged over ω = 0.6 to 3 rad/s for a constant oscillation displacement of 0.1 rad, and (c) Wi. The dashed line shows the correlation of Owolabi et al.[18], and the solid line shows a linear fit: $DR'_0=175\times(G'/G'')-73$.

V. SUMMARY AND CONCLUSION

The relationship between drag reduction (DR) and the rheology of polyacrylamide (PAM), polyethylene oxide (PEO), xanthan gum (XG), and carboxymethyl cellulose (CMC) solutions was experimentally investigated. Each polymer solutions was prepared at a different concentration to produce the same shear viscosity at high shear rates. This methodology was chosen to isolate the effect of high-shear viscosity. The viscoelastic properties of the polymer solutions were investigated using a capillary break-up extensional rheometer (CaBER) and small-amplitude oscillatory shear measurements.

The DR performance of each solution and its mechanical degradation was measured in a turbulent pipe flow at Re = 20,600, based on bulk velocity and pipe diameter. The flexible polymers (PAM and PEO) produced larger DR than the rigid polymers (XG and CMC). Drag reduction of PEO quickly reduced to zero due to mechanical degradation, while XG and CMC demonstrated negligible mechanical degradation. Drag reduction and mechanical degeneration were both independent of shear viscosity at low and high shear rates.

The viscoelasticity of the polymer solutions in weak and strong flows were characterized using oscillatory shear viscosity and CaBER measurements, respectively. The drag reduction correlated with the relaxation time and Weissenberg number (Wi) obtained from CaBER measurements. We did not observe a strong correlation between the elastic and viscous moduli obtained from the small-amplitude oscillatory shear measurements and drag reduction. CaBER measurements also showed increase of the extensional viscosity with decreasing strain rate for PEO. For PEO, this process continued until filament breakup and is hypothesized to result in its larger mechanical degradation. For other polymer filaments, the extensional thickening behavior is followed by a Newtonian regime in which extensional viscosity increased with increasing strain rate.

AKNOWLEDGEMENTS

The authors gratefully acknowledge financial support provided by Natural Sciences and Engineering Research Council of Canada (NSERC), Alberta Innovates-Technology Futures (AITF), Sadler Scholarship in Mechanical Engineering, and the Donald Lougheed Engineering Graduate Scholarship. In addition, the authors recognize Dr. Bayode Owolabi and Dr. Japan Trivedi for their contributions to the extensional viscosity measurements.

VI. References

[1] W.J. Han, and H.J. Choi, "Role of Bio-Based Polymers on Improving Turbulent Flow Characteristics: Materials and Application," Polymers 9, 209, 1 (2017).

[2] M.D. Warholic, D.K. Heist, M. Katcher, T.J. Hanratty, "A study with particle-image velocimetry of the influence of drag-reducing polymers on the structure of turbulence," Experiment in Fluids 31, 474 (2001).

[3] P.S. Virk, "Drag reduction fundamentals," American Institute of Chemical Engineers Journal 21, 625 (1975).

[4] J.W. Hoyt, Drag reduction by Polymers And Surfactants," American Institute of Aeronautics and Astronautics, 413 (1989).

[5] A. Abubakar, T. Al-Wahaibi, Y. Al-Wahaibi, A.R. Al-Hashmi, A. Al-Ajmi, "Review, Roles of drag reducing polymers in single- and multi-phase flows," Chemical Engineering Research and Design 92, 2153 (2014).

[6] W. Interthal, H. Wilski, "Drag reduction experiments with very large pipes," Colloid and Polymer Science 263, 217 (1985).

[7] A.S. Pereira, E.J. Soares, "Polymer degradation of dilute solutions in turbulent drag reducing flows in a cylindrical double gap rheometer device," Journal of Non-Newtonian Fluid Mechanics 179–180, 9 (2012).

[8] A.S. Pereira, R.M. Andrade, E.J. Soares, "Drag reduction induced by flexible and rigid molecules in a turbulent flow into a rotating cylindrical double gap device: Comparison between Poly (ethylene oxide), Polyacrylamide, and Xanthan Gum," Journal of Non-Newtonian Fluid Mechanics 202, 72 (2013).

[9] P.S. Virk, Drag reduction by collapsed and extended polyelectrolytes. Nature, 253(5487), 109-110, (1975).

[10] A. Japper-Jaafar, M.P. Escudier, R.J. Poole, Turbulent pipe flow of a drag-reducing rigid "rod-like" polymer solution. Journal of Non-Newtonian Fluid Mechanics, 161(1-3), 86-93 (2009).

[11] P.S. Virk, and D.L. Wagger. "Aspects of mechanisms in type B drag reduction." In Structure of turbulence and drag reduction, pp. 201-213. Springer, Berlin, Heidelberg, 1990.

[12] J.L. Lumley, "Drag reduction by additives," Annual Review of Fluid Mechanics 1(1), 367 (1969).

[13] H. Teng, N. Liu , X. Lu and B. Khomami, “Turbulent drag reduction in plane Couette flow with polymer additives: a direct numerical simulation study,” Journal of Fluid Mechanics 846, 482 (2018).

[14] C.M White, M.G. Mungal, “Mechanics and prediction of turbulent drag reduction with polymer additives,” Annual Review of Fluid Mechanics 40, 235 (2008).

[15] P.G. De Gennes, “Towards a scaling theory of drag reduction,” Physica 140A, 9 (1986).

[16] M.P. Escudier, F. Presti, S. Smith, “Drag reduction in the turbulent pipe flow of polymers,” Journal of Non-Newtonian Fluid Mechanics 81, 197 (1999).

[17] P. Dontula, M. Pasquali, L.E. Scriven, and , C.W. Macosko, ”Can extensional viscosity be measured with opposed-nozzle devices?,” Rheologica Acta, 36(4), 429 (1997).

[18] V. Entov, E. Hinch, “Effect of a spectrum of relaxation times on the capillary thinning of a filament of elastic liquid,” Journal of Non-Newtonian Fluid Mechanics 72, 31 (1997).

[19] B.E. Owolabi, D.J.C. Dennis, and R.J. Poole, “Turbulent drag reduction by polymer additives in parallel-shear flows,” Journal of Fluid Mechanics Rapids 827, 1 (2017).

[20] T. Nakken a, M. Tande, A. Elgsaeter, “Measurements of polymer induced drag reduction and polymer scission in Taylor flow using standard double-gap sample holders with axial symmetry,” Journal of Non-Newtonian Fluid Mechanics 97, 1 (2001).

[21] M.P. Escudier, I.W. Gouldson, A.S. Pereira, F.T. Pinho, R.J. Poole, “On the reproducibility of the rheology of shear-thinning liquids,” Journal of Non-Newtonian Fluid Mechanics 97, 99 (2001).

[22] N.B. Wyatt, C.M. Gunther, M.W. Liberatore,” Drag reduction effectiveness of dilute and entangled xanthan in turbulent pipe flow,” Journal of Non-Newtonian Fluid Mechanics 166, 25 (2011).

[23] S.A. Vanapalli, S.L. Ceccio, and M.J. Solomon. “Universal scaling for polymer chain scission in turbulence,” Proceedings of the National Academy of Sciences of the United States of America, 103, 16660 (2006).

[24] M.P. Escudier, A.K. Nickson, R.J. Poole, “Turbulent flow of viscoelastic shear-thinning liquids through a rectangular duct: Quantification of turbulence anisotropy,” Journal of Non-Newtonian Fluid Mechanics 160, 2 (2009).

[25] E.J. Soares, G.A.B. Sandoval, L. Silveira, A.S. Pereira, R. Trevelin, and F. Thomaz, “Loss of efficiency of polymeric drag reducers induced by high Reynolds number flows in tubes with imposed pressure,” Physics of Fluids 27, 125105 (2015).

[26] R. Vonlanthen and P.A. Monkewitz, “Grid turbulence in dilute polymer solution: PEO in water,” Journal of Fluid Mechanics 730, 76 (2013).

[27] Y.A. Çengel, J.M. Cimbala,” Fluid mechanics: fundamentals and applications,” (3st ed.). New York: McGraw-Hill, p.353 (2014).

[28] M. Mohammadtabar, R.S. Sanders, and S. Ghaemi, "Turbulent structures of non-Newtonian solutions containing rigid polymers," Physics of Fluids 29, 103101 (2017).

[29] P.K. Ptasinski, B.J. Boersma, F.T.M. Nieuwstadt, M.A. Hulsen, B.H.A.A. Van Den Brule, and J.C.R. Hunt, "Turbulent channel flow near maximum drag reduction: simulations, experiments and mechanisms," Journal of Fluid Mechanics 490, 251 (2003).

[30] O. BASF- the chemical company, "Magnafloc® 5250- mining solutions- BASF corporation," Product Brochure TI/EVH 0033 e , 1 (March 2013).

[31] Kemira, "Superfloc® Flocculants & Coagulants," Product Brochure V9.4.

[32] SIGMA-ALDRICH, "Product specification- poly (ethylene oxide)- average Mv ~ 8,000,000, powder," Product Brochure.

[33] M. Papagianni, S.K. Psomas, L. Batsilas, S.V. Paras, D.A. Kyriakidis, and M. Liakopoulou-Kyriakides, "Xanthan production by Xanthomonas campestris in batch cultures," Process Biochemistry, 37, 73 (2001).

[34] T. Siritientong, and P. Aramwit, "Characteristics of Carboxymethyl Cellulose/Sericin Hydrogels and the Influence of Molecular Weight of Carboxymethyl Cellulose," Macromolecular Research, Vol. 23, No. 9, pp 861-866 (2015).

[35] G. Schramm, "A practical approach to rheology and rheometry (p. 162, 167, 171)," Karlsruhe: Haake (1994).

[36] Thermo Scientific, "Instruction Manual, HAAKE CaBER 1" Thermo Electron (Karlsruhe) GMBH, Product Brochure V1.8 (2006).

[37] F. Olsson, J. Ystrom, "Some properties of the Upper Convected Maxwell model for viscoelastic fluid flow" Journal of Non-Newtonian Fluid Mechanics, 48, 125 (1993).

[38] E. Miller, C. Clasen, & J. P. Rothstein, "The effect of step-stretch parameters on capillary breakup extensional rheology (CaBER) measurements." Rheologica Acta, 48, 625 (2009)

[39] S.L. Anna, G.H. McKinley, "Elasto-capillary thinning and breakup of model elastic liquids," Journal of Rheology 45, 115 (2001).

[40] S. Shaban, M. Azad, J. Trivedi, and S. Ghaemi. Investigation of near-wall turbulence in relation to polymer rheology. Physics of Fluids, 30(12), 125111, (2018).

[41] M.P. Escudier, A.K. Nickson, R.J. Poole, "Turbulent flow of viscoelastic shear-thinning liquids through a rectangular duct: Quantification of turbulence anisotropy," Journal of Non-Newtonian Fluid Mechanics 160, 2 (2009).

[42] J. Dinic, Y. Zhang, L.N. Jimenez, and V. Sharma, "Extensional Relaxation Times of Dilute, Aqueous Polymer Solutions," ACS Macro Letters, 4, 804 (2015).

[43] D.T. Papageorgiou. On the breakup of viscous liquid threads. Physics of fluids, 7(7), 1529-1544, (1995).

[44] V.M. Entov, and E. J. Hinch. Effect of a spectrum of relaxation times on the capillary thinning of a filament of elastic liquid. Journal of Non-Newtonian Fluid Mechanics, 72(1), 31-53, (1997).

[45] E.E.B. White, M. Chellamuthu, and J.P. Rothstein. Extensional rheology of a shear-thickening cornstarch and water suspension. Rheologica Acta, 49(2), 119-129, (2010).

[46] A. K. Townsend, and H. J. Wilson. Small-and large-amplitude oscillatory rheometry with bead–spring dumbbells in Stokesian Dynamics to mimic viscoelasticity. Journal of Non-Newtonian Fluid Mechanics, 261, 136-152, (2018).

[47] G. H. McKinley, T. Sridhar. Filament-stretching rheometry of complex fluids. Annual Review of Fluid Mechanics, 34(1), 375-415, (2002).

[48] S. Rogers. Large amplitude oscillatory shear: Simple to describe, hard to interpret. Physics Today, 71(7), 34-40, (2018).